Resonant Raman scattering and piezomodulated reflectivity of InP in high magnetic fields

T. Ruf, R. T. Phillips,* A. Cantarero,† G. Ambrazevičius,‡ and M. Cardona
Max-Planck-Institut für Festkörperforschung, Heisenbergstrasse 1, D-7000 Stuttgart 80, Federal Republic of Germany

J. Schmitz
Institut für Theoretische und Angewandte Physik, Universität Stuttgart, D-7000 Stuttgart 80, Federal Republic of Germany

U. Rössler
Institut für Theoretische Physik, Universität Regensburg, D-8400 Regensburg, Federal Republic of Germany
(Received 26 January 1989)

In a magnetic field the efficiency for Raman scattering by LO phonons in InP(001) exhibits resonant structure which can be associated with interband magneto-optical transitions between Landau levels. The Raman processes are found to occur in outgoing resonance and theoretical transitions, determined by an 8×8 $\mathbf{k}\cdot\mathbf{p}$ calculation, are assigned to the experimental fan lines. A model for the Raman processes is deduced which explains the resonances in different scattering configurations with circularly polarized light using deformation-potential and Fröhlich electron-phonon interaction in a heavily mixed valence band. To substantiate the theoretical description of the Raman processes by obtaining directly the interband transitions, piezoreflectance measurements are performed. For conduction-band Landau levels E_n around $E_0+\hbar\Omega(\mathrm{LO})$, pronounced anticrossings are found which can be attributed to resonant magnetopolaron effects. No anticrossings other than with the $|n=0,\ 1\text{-LO}\rangle$ state are observed in the reflectivity measurements which were performed up to 18.5 T. In the Raman data, however, anticrossings with higher Landau levels up to $|n=2,\ 1\text{-LO}\rangle$ are found.

I. INTRODUCTION

Interband magneto-optical studies of semiconductors provide a powerful tool to obtain band-structure information about this technologically important class of materials.[1] Together with elaborate theories, they can be used for a highly accurate determination of band parameters.[2–8] Recently it was demonstrated that resonant Raman scattering by LO phonons between Landau levels can be used to enhance our knowledge of the conduction-band nonparabolicity of GaAs.[9]

In the attempt to apply this technique to InP in the region above the E_0 gap, we encountered several phenomena which have to be taken into account in order to arrive at a consistent description of resonant Raman scattering in a magnetic field:[10] Valence-band mixing has to be considered explicitly within the $\{\Gamma_6^c,\Gamma_8^v,\Gamma_7^s\}$ manifold to describe the complex selection rules which are found in the scattering configurations with circularly polarized light. Corrections for the exciton binding energies have to be used since our experiments were performed in a region of small oscillator quantum numbers ($n<10$). Finally, resonant magnetopolaron effects introduce pronounced anticrossings in the fan lines whenever the energy difference between two conduction-band Landau levels becomes equal to the energy of the LO phonon.

Resonant Raman scattering for laser energies up to 200 meV above the E_0 gap was found to occur in outgoing resonance channels. The energy of one LO phonon has thus to be subtracted from the laser energy in order to compare the experiment with theoretical interband transitions. To obtain direct experimental information about the interband transitions, we measured the piezomodulated reflectivity spectra (piezoreflectance).[1] The results provide a thorough test of our theoretical model before we apply it to the more complicated Raman processes which are described by third-order perturbation theory.

This paper is organized as follows. In Sec. II we give a brief description of the experimental techniques. The theory is discussed in Sec. III. In Sec. IV we present the piezoreflectance data and discuss the most important interband magneto-optical transitions. Section V is devoted to the Raman data. A model for resonant Raman scattering involving Landau levels in InP is introduced which explains the spectra obtained in different scattering configurations. The resonant magnetopolaron effects are discussed in both Secs. IV and V for the two types of experiments. A summary of the results and new aspects of this work is given in Sec. VI.

II. EXPERIMENT

The experiments were performed on two samples of InP with (001) surfaces: The Raman data for laser energies up to 1.56 eV were measured on a metalorganic chemical-vapor-deposition (MOCVD) -grown sample with $n=1.4\times10^{15}$ cm^{-3} and $\mu_{77}=45\,500$ cm^2/V s provided by Scholz.[11] To measure the Raman oscillations at higher incident laser energies (1.55–1.63 eV) and to obtain higher-resolution reflectivity data, we found it neces-

sary to use a very-high-purity MOCVD-grown sample of InP with $n=3\times10^{13}$ cm^{-3} and $\mu_{77}=268{,}000$ cm^2/V s provided to us by Thrush.[12] The Raman data from the two specimens were compared for laser energies around 1.55 eV; agreement in all details was found. The piezoreflectance measurements, however, were performed on the higher-mobility material over the whole range of energies because of the increased sharpness with which the interband transitions show up in the first-derivative spectra.

The Raman data were obtained in the Faraday configuration with a split-coil superconducting magnet which provides fields up to $B=12.8$ T.[9,10] For each laser energy a Spex 1404 double monochromator is set at a fixed energy corresponding to the Stokes-Raman LO-phonon peak ($\hbar\omega_L-43$ meV) and operated as a spectral bandpass with a width of 1 meV. The signal, retrieved with a GaAs-photomultiplier (RCA C31034A, cooled to -50 °C) and conventional photon-counting electronics, provides a measure of the Raman-scattering efficiency. This efficiency is then measured as a function of the magnetic field for the four different scattering configurations with circularly polarized light. The experiments were performed in an exchange-gas cryostat with a sample temperature of about 10 K.

The piezoreflectance spectra[1,13] were measured up to 18.5 T generated by a Bitter magnet. A unipolar modulation voltage ($f=400$ Hz, $V_{p\text{-}p}=275$ V) from a Kepco high-voltage operational amplifier was applied to a PXE 5 piezoelectric transducer[14] with a thickness of 0.3 mm. The sample was mounted onto the transducer using conductive carbon cement[15] which allows for good transmission of the strain into the specimen. The sample was illuminated with white light from a 150-W quartz-iodine tungsten lamp and the reflected radiation was dispersed with a Jobin-Yvon HRS1 single monochromator. A Si photodiode with integrated field-effect transistor (FET) amplifier[16] and conventional phase-sensitive detection were used to retrieve the signal. The measurements were performed in a He-bath cryostat so that the sample temperature was slightly lower than in the Raman experiments. From the spectrum of the E_0 exciton at $B=0$, it was made sure that the specimen was not strained[17] due to the mounting onto the piezoelectric transducer.

III. THEORY

It was realized early by Luttinger and Kohn[2,3] that the degeneracy of the valence-band edge in diamond-type semiconductors leads to a series of irregularly spaced Landau levels when a magnetic field is present. Only in the limit of large oscillator quantum numbers are two equally spaced series for heavy and light holes found. Pidgeon and Brown[4] extended the Luttinger-Kohn formalism to zinc-blende-type semiconductors (similar to diamond but without a center of inversion) and at the same time treated the conduction band on the same footing as the valence and spin-orbit split-off bands. Using an invariant-expansion formalism[18] which was applied to the case of diamond-type semiconductors under uniaxial stress in a magnetic field, by Suzuki and Hensel,[19,20] Trebin and Rössler[5–8] treated this problem for zinc-blende semiconductors. The set of $\{\Gamma_6^c,\Gamma_8^v,\Gamma_7^s\}$-basis functions is considered quasidegenerate and interactions within and between the Γ_6^c conduction band and the Γ_8^v and the Γ_7^s bands are handled in an exact way, while interactions with more remote bands are treated by second-order perturbation theory. In an invariant expansion the Hamiltonian is split into terms of different symmetries. This symmetry classification leads to a hierarchy of axial, cubic, and tetrahedral contributions.[5] The eigenstates within the eightfold space can then be characterized by sets of quantum numbers which correspond to the respective symmetry of parts of the Hamiltonian. In the Pidgeon-Brown model only the terms of highest axial symmetry are treated exactly, the terms of lower symmetry are treated as a perturbation. Using the concept of invariant expansion, selection rules for interband transitions can be obtained on purely group-theoretical grounds. The strength with which allowed transitions occur is determined by material constants. It is found to be weaker for terms of lower symmetry.

For a magnetic field in the [001] direction and terms of axial symmetry, an eigenstate is described by a set of quantum numbers N_n,K^π,Q,P.[5] $N=n+m_J+\frac{3}{2}$ is the quantum number of axial symmetry ($C_{\infty h}$). It corresponds to the z component of total angular momentum to which the cyclotron motion (Landau quantum number n) contributes, as well as the equivalent angular momentum of the Bloch state ($J=\frac{3}{2}$ for Γ_8^v and $J=\frac{1}{2}$ for Γ_6^c and Γ_7^s). If cubic terms are considered, the axial symmetry is reduced to C_{4h} (for $\mathbf{B}\|[001]$) and the eigenstates are labeled by $K=N$ mod 4. For $k_z\cong0$, the dominant case for dipole transitions, a parity π can be assigned to the eigenstates. Including tetrahedral terms with $k_z=0$ lowers the symmetry from C_{4h} to S_4 (states being labeled by $Q=0,1,2,3$), while tetrahedral terms with $k_z\neq0$ are invariant only under C_2 (states being labeled by $P=0,1$). The selection rules of importance for our case can be summarized by $\Delta N=\pm1$, $\Delta\pi=\pm1$, $\Delta K=\pm1$, and $\Delta P=1$ (Ref. 5) for σ^+ (σ^-) circularly polarized interband transitions induced by the stronger terms of axial symmetry. The less stringent selection rule $\Delta P=1$ (mod 2) holds for the transitions mediated by the weaker tetrahedral terms. For convenience, we are going to label the eigenstates with the more instructive notation $|n,\{S,V,C\},m_J\rangle$. Here S, V, or C stand for the split-off, valence, or conduction bands with $J=\frac{1}{2},\frac{3}{2},\frac{1}{2}$, respectively. We shall only refer to the explicit description in terms of the N_n,K^π,Q,P quantum numbers, which can be derived from the above notation when necessary.

So far, we have described the uncorrelated electron and hole states appropriate to the interpretation of our experiments. The eigenvalues and eigenvectors are obtained by numerically[21] solving their Hamiltonian. They can be used to interpret interband magneto-optical transitions. However, it was realized early[22] that electron-hole Coulomb attraction plays an important role. Unfortunately, an exact solution of a Hamiltonian which includes band effects, magnetic field, and Coulomb attraction has not yet been obtained. There are, however, ap-

proximations for the cases when the cyclotron energy is large compared to the Coulomb energy[22–24] and *vice versa*.[23,25] In these calculations one of the two effects is treated exactly and the other as a perturbation. The reduced magnetic field γ, defined by $\gamma=\hbar\omega_c^*/2R_0^*$ where $\hbar\omega_c^*=\hbar eH/\mu$ is the effective cyclotron energy and $R_0^*=\mu e^4/2\hbar^2\epsilon^2$ is the effective Rydberg, is used to characterize the high-field limit in which $\gamma\gg1$.[24] For InP this is the case for magnetic fields above 7 T. We obtain the exciton ground-state binding energies as a correction to the Landau levels by solving the one-dimensional Schrödinger equation

$$\left[-\frac{\hbar^2}{2\mu}\frac{d^2}{dz^2}+V(z)\right]f(z)=Ef(z)\ , \tag{1}$$

which is based on the assumption that for high magnetic fields the Coulomb interaction only affects the electron motion in the direction of the magnetic field.[22] It is, however, not possible to solve this equation with the full Coulomb potential. A potential of the general form

$$V(z)=-\frac{e^2}{\epsilon(a_0^*a_n+|z|)},\quad a_0^*=\frac{\hbar^2\epsilon}{\mu e^2} \tag{2}$$

can be used to approximate the Coulomb potential where the a_n have to be chosen for each Landau oscillator quantum number n.[22] We find that the choice $a_n=\sqrt{(2n+1)/\pi\gamma}$ gives an excellent approximation to the adiabatic potentials which were obtained by Baldereschi and Bassani[23] by numerical integration of the Schrödinger equation with the full Coulomb potential.

We now solve Eq. (1) with a variational method using the approximate potential (2). With the ansatz

$$f(z)=\sqrt{\beta}e^{-\beta|z|}\ , \tag{3}$$

we arrive at the condition

$$-\frac{x}{4a_n}=1+(1+x)e^x\mathrm{Ei}(-x),\quad x=2\beta a_0^*a_n \tag{4}$$

for the variational parameter β which optimizes the exciton binding energy E, where $\mathrm{Ei}(-x)$ is the exponential integral function.[26] For Landau oscillator quantum number n, the binding energy of the exciton ground state is then given by

$$E(\bar{x})=\left[\left(\frac{\bar{x}}{2a_n}\right)^2-\frac{\bar{x}}{2a_n}\frac{4a_n+\bar{x}}{a_n(1+\bar{x})}\right]R_0^*\ , \tag{5}$$

where $\bar{x}$ is the solution of (4). With this approach, the results of Larsen[27] can be reproduced with good accuracy.

The theory outlined above is necessary to understand the interband magneto-optical transitions mediated by the electron-photon interaction. Because of its complexity and the multitude of transitions which can be calculated, we find it mandatory to test the theoretical picture by comparing it to results obtained from piezo-magnetoreflectance measurements before reliable statements about the more complicated resonant Raman process can be made. The efficiency for resonant Raman scattering is given in third-order perturbation theory by the expression[28,29]

$$W_{if}\sim\left|\sum_{|n\rangle,|m\rangle}\frac{\langle f|H_{e\text{-phot}}|n\rangle\langle n|H_{e\text{-phon}}|m\rangle\langle m|H_{e\text{-phot}}|i\rangle}{(\hbar\omega_S-E_n+i\Gamma_n)(\hbar\omega_L-E_m+i\Gamma_m)}\right|^2, \tag{6}$$

where $|n\rangle,|m\rangle$ are intermediate states of energy E_n,E_m and lifetime broadening Γ_n,Γ_m. $|i\rangle$ and $|f\rangle$ denote initial and final states; $\hbar\omega_L$ and $\hbar\omega_S$ are the energies of the exciting laser and the scattered radiation, where the relation $\hbar\omega_L=\hbar\omega_S+\hbar\Omega_{\text{phon}}$ holds, $\hbar\Omega_{\text{phon}}$ being the energy of the phonon emitted in the process. $H_{e\text{-phot}}$ denotes the electron-photon interaction, $H_{e\text{-phon}}$ that between electrons and phonons. There are two matrix elements from interband magneto-optical transitions which enter into the expression for the Raman-scattering efficiency. At this point we are going to use the results of the theory outlined above in the interpretation of our experiments: The two denominators, which can cause an enhancement of the Raman efficiency in incoming ($\hbar\omega_L$) and outgoing ($\hbar\omega_S$) resonance, provide the connection between calculated transition energies and the experiment, whereas the matrix elements can be used to sort out selection rules.

However, for a complete description of the Raman process, the matrix element and the selection rules for the electron-phonon interaction have to be known. There have been a few studies of the electron-phonon interaction in a magnetic field treating the Fröhlich interaction in a simple free-electron model (for the purpose of describing cyclotron resonance).[30–33] It was shown that the Fröhlich Hamiltonian couples Landau states with arbitrary oscillator quantum numbers n.[30] In an eight-band model, including spin-orbit interaction, an additional selection rule for the component of the total angular momentum in the direction of the magnetic field holds, which arises from the Bloch part of the wave functions.[2,5,34] Thus the Fröhlich Hamiltonian only couples equal Bloch states. The deformation-potential electron-phonon interaction leads to nonvanishing matrix elements between Landau levels with the same oscillator quantum numbers. In the valence bands the Bloch parts of the wave functions give the usual couplings of $|J=\frac{3}{2},\pm\frac{3}{2}\rangle$ to $|J=\frac{3}{2},\mp\frac{1}{2}\rangle$ and $|J=\frac{1}{2},\mp\frac{1}{2}\rangle$ states.[29] With these selection rules we can describe possible resonant enhancements in the Raman efficiency. A detailed calculation of the one-photon resonant Raman processes in a magnetic field, including both Fröhlich and deformation-potential electron-phonon interaction will be published later.[35]

Other phenomena related to Fröhlich interaction in polar semiconductors are resonant magnetopolaron effects which occur whenever harmonics of the cyclotron

frequency in the conduction band are equal to the energy of a LO phonon.[36–40] In a simple picture, the Fröhlich interaction causes an anticrossing of Landau levels in the resonant region where a $|n,1\text{-LO}\rangle$ state becomes degenerate with an $|n+\Delta n,0\text{-LO}\rangle$ state. As the magnetic field is increased towards resonance, the lower $|n+\Delta n,0\text{-LO}\rangle$ state loses its oscillator strength and the fan line bends such that its slope approaches that of the higher $|n,1\text{-LO}\rangle$ state. At the same time, and for higher magnetic fields, the $|n,1\text{-LO}\rangle$ state picks up oscillator strength and the fan line bends up towards that of the lower $|n+\Delta n,0\text{-LO}\rangle$ state. This upper branch, however, is degenerate with the k_z-dependent continuum of the lower Landau states. Thus it is strongly broadened due to emission of LO phonons[39] and it is difficult to observe it in interband experiments.

The splitting at the anticrossing depends on the Fröhlich constant α and thus on the polarity of the material under investigation. For InP we have $\alpha=0.11$ (Ref. 41) and the anticrossing energy, which is given by $\pm\alpha\hbar\Omega(\text{LO})$, is almost 10 meV. This is twice as much as for GaAs;[39,41] thus InP is a very suitable material with which to study these effects.

IV. INTERBAND MAGNETOREFLECTIVITY

Figure 1 shows typical piezoreflectance spectra of InP(001) at liquid-He temperature for several magnetic fields. With our better sample we obtained high-resolution spectra which show more interband magneto-optical features than have been observed before.[42] We see at first glance a series of closely spaced features, weaker than the more pronounced structures labeled $A-G$. In a simplistic approach these two types of features can be regarded as the heavy- and light-hole ladders.[2–5] In order to assign peak positions in a consistent way, we chose as excitation energies the negative extrema on the lower-energy side of each structure. Due to the sharpness of the features in our high-resolution spectra, these values do not deviate significantly from the actual critical energies, which for first-derivative Lorentzian spectra correspond to the zero between negative and positive extrema, by more than 0.5 meV. These possible offsets should be about the same for all structures. In order to assign the observed peaks we calculate Landau levels and interband transition energies for each magnetic field. Among the various sets of Luttinger parameters found in the literature,[41,43,44] best agreement is found using those of Table I. All mass parameters include a renormalization due to the Fröhlich interaction (except the resonant one discussed above). The Luttinger parameters γ_1 and γ_2 are close to those used in recent calculations.[43] The anisotropy of the $|\frac{3}{2},\pm\frac{3}{2}\rangle$ states, expressed by the difference between γ_2 and γ_3, which is smaller in Ref. 43, is essential to obtain the strong valence-band mixing needed to interpret the Raman data (see below). This anisotropy, however, does not affect the transition energies within the experimental accuracy. A recent determination of γ_3 using hot photoluminescence[44] supports the present value. Terms linear in $\mathbf{k}$, expressed by the constant C, do not yield observable changes in the transition energies when

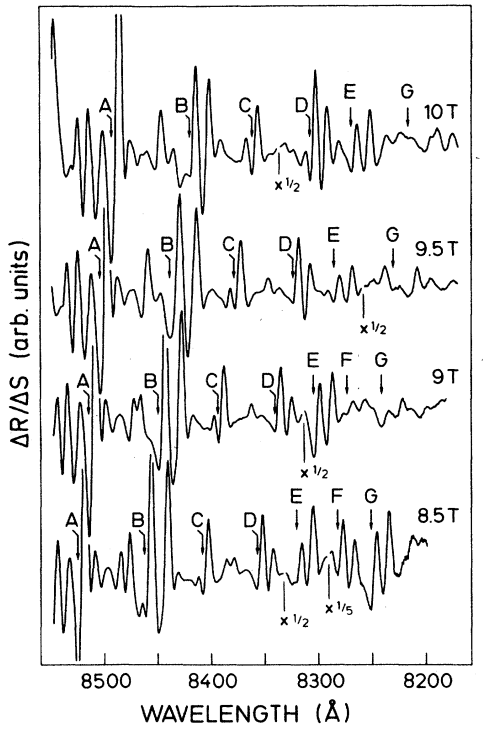

FIG. 1. Piezoreflectance spectra of InP(001) for different magnetic fields. The features labeled $A-G$ are interband magneto-optical transitions involving $|J=\frac{3}{2},\pm\frac{3}{2}\rangle$ valence-band states. The sign of ΔR corresponds to a tensile biaxial stress. It was determined from the effect on the main exciton for $B\simeq 0$.

varied around reported values.[43] The most striking result of the calculation is that the valence-band states become strongly mixed, i.e., one can no longer consider pure heavy- and light-hole states. The implications of this valence-band mixing on the description of the Landau levels in terms of a single effective mass have been pointed out.[45] The calculations give particularly strong interband transitions whenever states with $|J=\frac{3}{2},\pm\frac{3}{2}\rangle$ as Bloch parts of the wave function become dominant in the admixtures of the corresponding valence Landau levels. The pronounced features in the spectra can be attributed to these transitions. The weaker structures correspond to a multitude of closely spaced possible transitions which have $|J=\frac{3}{2},\pm\frac{1}{2}\rangle$ Bloch states as dominant constituents. Table II shows the interband transitions which we assign to the features labeled $A-G$ in Fig. 1. To characterize the valence-band state of a particular transition, we use its strongest component. A consistent picture emerges: For each Landau oscillator quantum number n there are two strong transitions, one with a change of m_J from $m_J=+\frac{3}{2}$ to $m_J=+\frac{1}{2}$ (features A,C,E,G) and another where m_J changes from $m_J=-\frac{3}{2}$ to $m_J=-\frac{1}{2}$ (features B,D,F). Since $\Delta m_J=\pm 1$ these transitions can be distinguished with circularly polarized light (see Sec. V). From the calculations it is found that for magnetic fields up to 18 T the conduction levels for the same Landau quantum number n should not split by more than 1.5

TABLE I. Parameters used to calculate Landau levels in InP.

Luttinger parameters[a]	Further band and gap parameters[b]	Band-interaction parameters[b]
$\gamma_1=4.95$	$1+2F=-1.75$	$P=8.88\times10^{-8}$ eV cm
$\gamma_2=1.65$	$g+4N_1=-1.956$	$B=-2.734\times10^{-16}$ eV cm^2
$\gamma_3=2.35$	$C=0.00$	$P'=8.88\times10^{-8}$ eV cm
$\kappa=0.97$	$E_0=1.423$ eV[a]	$B'=-2.684\times10^{-16}$ eV cm^2
$q=0.00$	$\Delta_0=0.110$ eV[a]	$N_2=-0.003$
		$N_3=-0.003$

[a]Reference 41.
[b]A description of the parameters is given in Refs. 5 and 47.

meV for the two states with spin up and down. The experiment, however, gives a much larger separation of the interband energies for transitions involving the same n but opposite spins. This can be understood only when the valence Landau levels are explicitly taken into account.

Subtraction of the theoretical valence contributions (see Fig. 2) from the experimental transition energies gives the conduction-band fan charts shown as dash-dotted lines in Fig. 3. The experimental energies are systematically found to be lower than the pure Landau levels (solid lines). A correction for excitonic effects (dashed lines), as outlined in Sec. III, is necessary to obtain a satisfactory description of the experiment.

Whenever harmonics of the cyclotron energy become equal to the energy of a LO phonon (43 meV in InP), anticrossings due to Fröhlich-interaction-mediated magnetopolaron resonances may occur.[36–40] This phenomenon can be observed in Fig. 1 for transitions F and G which become weaker and broader for increasing magnetic fields. Table II shows deviations between the experimental and theoretical (exciton corrected) transition energies for features $D-G$. In Fig. 3 we find a clear pinning of the interband transition energies to the $|n=0,C,\pm\frac{1}{2};1\text{-LO-phonon}\rangle$ Landau levels when the magnetic field becomes high enough for the resonances to occur. Anticrossings at magnetic fields corresponding to the second to fourth harmonic of the cyclotron frequency are observed. As mentioned in Sec. III, the upper branches of the anticrossings are hardly observed due to the admixture of states from the k_z continuum of the lower Landau levels which leads to broader and weaker transitions. By comparing the observed anticrossings to the lines calculated without electron-phonon interaction, we estimate the energy separation between the upper and lower branches to be about 6 meV. This leads to a Fröhlich coupling constant of $\alpha=0.07\pm0.01$ somewhat smaller than the literature value of $\alpha=0.11$.[41] A peculiar behavior is found for transition A, which shows strong bending at about 16 T, whereas neighboring peaks at slightly higher energies move straight on. This cannot be understood in the framework of our present theory. Valence-band effects may play a certain role since the energy of the valence-band contribution is the most pronounced difference between transition A ($|1,V,+\frac{3}{2}\rangle\rightarrow|1,C,+\frac{1}{2}\rangle$) and the partner transition $|1,V,-\frac{3}{2}\rangle\rightarrow|1,C,-\frac{1}{2}\rangle$, which does not show any deviations from linearity up to 18.5 T.

V. MAGNETO-RAMAN EXPERIMENTS

In Fig. 4 we show the intensity of the Stokes-Raman LO-phonon peak of InP(001) versus B, measured at a laser energy of $\hbar\omega_L=1.525$ eV for the four scattering configurations with circularly polarized light. The spectra for the two configurations with crossed polarizations mutually exclude each other, whereas those taken with

TABLE II. Assignment of theoretical interband magneto-optical transitions to the large features in the reflectivity spectra for a magnetic field of 9 T (see Figs. 1 and 3). Note the increasing difference between the experimental and the corrected theoretical transition energies for features $D-G$. They arise from resonant magnetopolaron interaction. All energies are given in meV.

Experiment			Theory			
Features	Transition energy	Transition	Transition energy	Valence-band contribution	Exciton correction	Corrected transition energy[a]
A	1456.2	$\|1,V,+\frac{3}{2}\rangle\rightarrow\|1,C,+\frac{1}{2}\rangle$	1461.1	18.5	4.4	1456.7
B	1467.4	$\|2,V,-\frac{3}{2}\rangle\rightarrow\|2,C,-\frac{1}{2}\rangle$	1471.4	16.9	3.6	1467.8
C	1477.2	$\|2,V,+\frac{3}{2}\rangle\rightarrow\|2,C,+\frac{1}{2}\rangle$	1480.6	25.5	3.6	1477.0
D	1486.6	$\|3,V,-\frac{3}{2}\rangle\rightarrow\|3,C,-\frac{1}{2}\rangle$	1491.1	24.3	3.2	1487.9
E	1493.0	$\|3,V,+\frac{3}{2}\rangle\rightarrow\|3,C,+\frac{1}{2}\rangle$	1499.6	32.1	3.2	1496.4
F	1498.6	$\|4,V,-\frac{3}{2}\rangle\rightarrow\|4,C,-\frac{1}{2}\rangle$	1510.0	31.0	2.9	1507.1
G	1504.4	$\|4,V,+\frac{3}{2}\rangle\rightarrow\|4,C,+\frac{1}{2}\rangle$	1517.9	38.3	2.9	1515.0

[a]Theoretical transition-energy–exciton correction.

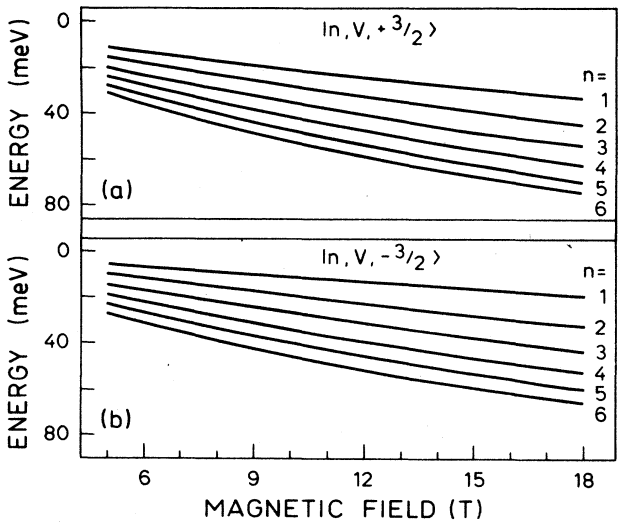

FIG. 2. Theoretical valence-band contributions used to correct the experimental data in Figs. 3 and 7. The valence Landau levels contribute to (a) $|n,V,+\frac{3}{2}\rangle \leftrightarrow |n,C,+\frac{1}{2}\rangle$ and (b) $|n,V,-\frac{3}{2}\rangle \leftrightarrow |n,C,-\frac{1}{2}\rangle$ interband transitions, respectively. The levels are labeled according to the dominant admixture in the wave function.

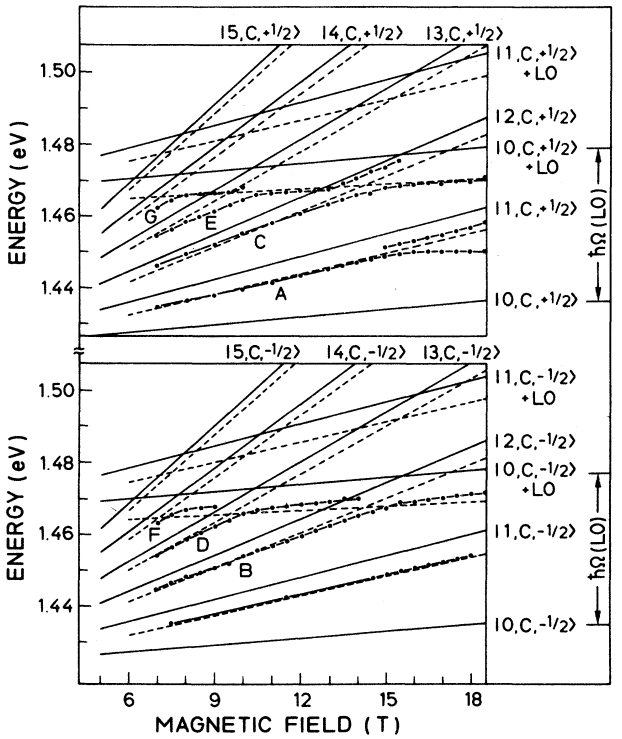

FIG. 3. Conduction-band contributions to interband magneto-optical transitions of InP(001) at liquid-He temperature: exciton and resonant magnetopolaron effects. Straight lines, theoretical Landau levels; dashed lines, theoretical Landau levels corrected for exciton binding energies; dashed-dotted lines, experimental transition energies after subtraction of theoretical valence-band contributions (see Fig. 2). Capital letters denote the transitions as given in Table II.

equal polarizations for both incident and scattered light show all the peaks which are found in the other two spectra. The resonant enhancement of the Raman efficiency compared to the intensity at zero field for the $\bar{z}(\sigma^+,\sigma^-)z$ and $\bar{z}(\sigma^-,\sigma^+)z$ spectra at $\hbar\omega_L = 1.525$ eV is larger than 40, whereas it is at least 4 times smaller in the $\bar{z}(\sigma^+,\sigma^+)z$ and $\bar{z}(\sigma^-,\sigma^-)z$ configurations. When one plots the peak positions found in the different spectra as $\hbar\omega_L$ versus B, it is realized that the fan lines do not converge to the E_0 gap as $B \rightarrow 0$, but rather they converge at an energy which is one LO-phonon energy above E_0. This indicates that the Raman processes occur in outgoing resonance, that is, the scattered photons correspond to real interband magneto-optical transitions. Thus the knowledge of the particular interband transitions which contribute to the Raman processes in outgoing resonance should yield important clues for the understanding of the dominant resonant Raman processes within the theoretical framework outlined in Sec. III.

In Fig. 5 the experimental fan lines for the four different scattering configurations are plotted as a function of B. On the energy scale we subtracted 43 meV from the laser energy for which the peaks occur to account for the fact that the resonance is outgoing. The resulting fan lines are found to be in agreement with the theoretical transition energies which we assigned to the dominant features of the piezoreflectance data in Sec. IV.

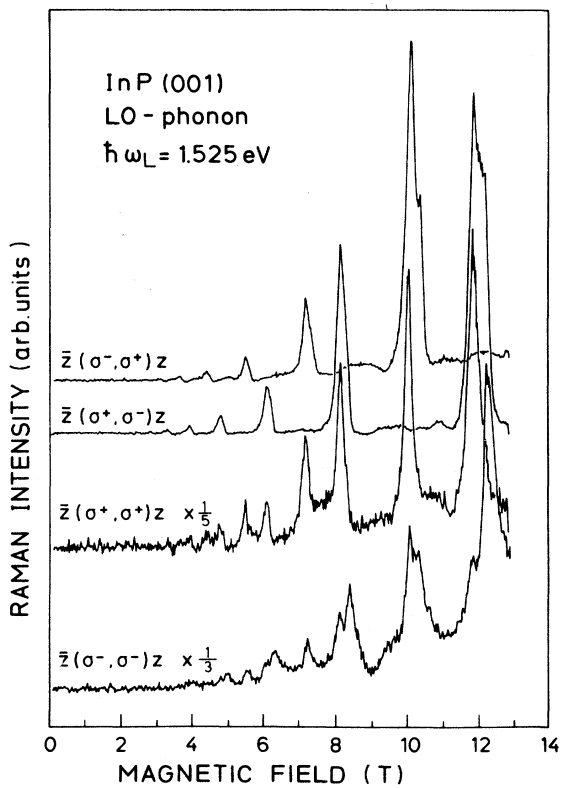

FIG. 4. Intensity of the Stokes-Raman LO-phonon peak vs magnetic field for InP(001) for the four different scattering configurations with circularly polarized light.

Corrections for exciton binding energies are incorporated in the calculated transition energies shown as straight lines in Fig. 5. The fan plots also show pronounced anticrossings which will be discussed later. The picture obtained from piezoreflectance data can now be applied to describe the Raman processes in outgoing resonance. Moreover, since we performed the Raman experiments with circularly polarized light, the previous assignment of transitions occurring in σ^+ and σ^- polarizations is verified by the Raman data.

Let us first concentrate on data taken with crossed polarizations. The experiments were performed with **B** pointing along $-\mathbf{z}$, whereas the opposite was assumed in the calculations.[5] This results in a complementary change of the circular polarization in which the theoretical interband transitions occur as compared to the experiment and has to be kept in mind.[46] The outgoing resonances in the $\bar{z}(\sigma^+,\sigma^-)z$-scattering configuration can be described by interband transitions between conduction-band states $|n,C,-\frac{1}{2}\rangle$ and valence-band Landau levels

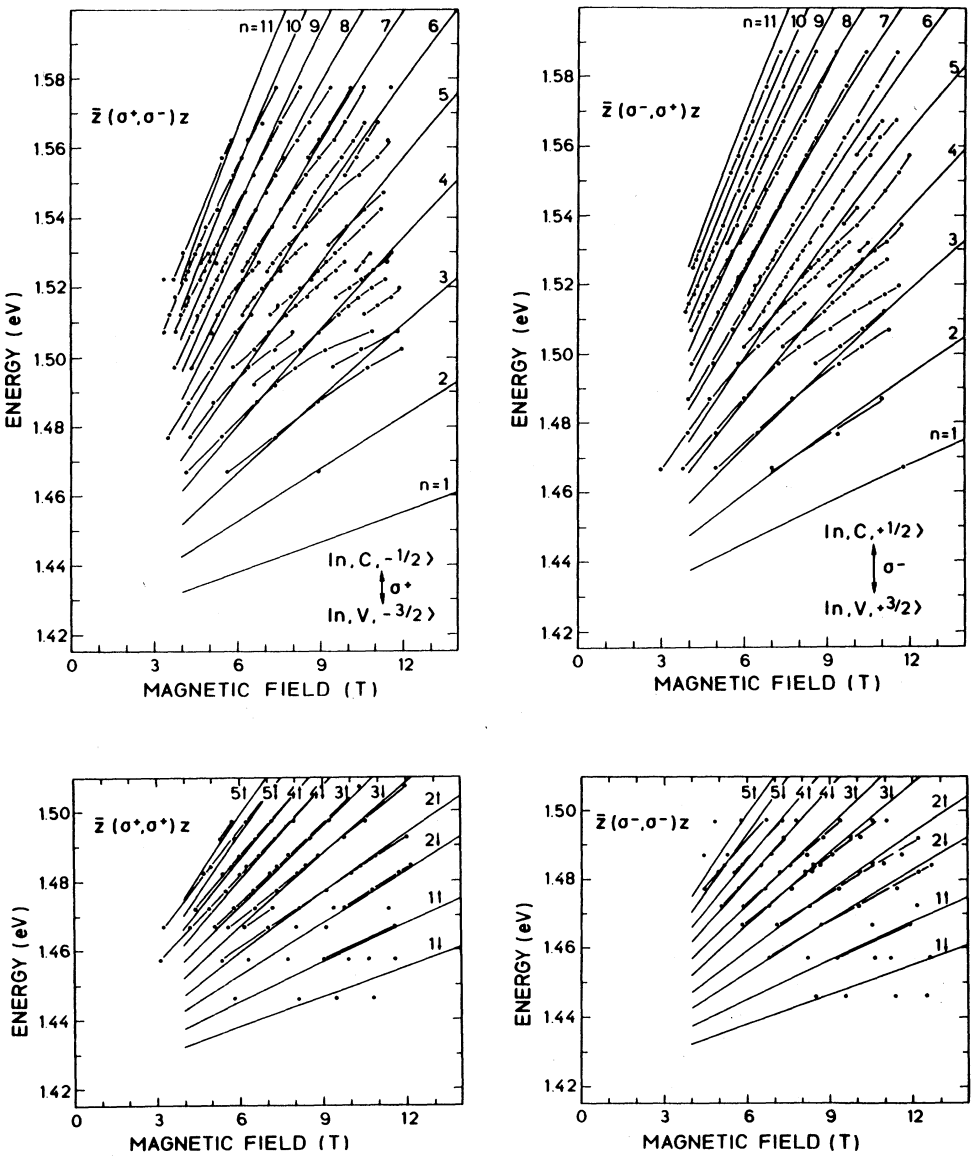

FIG. 5. Peaks in the Raman intensity vs magnetic field for the four scattering configurations possible with circularly polarized light. The straight lines indicate theoretical transition energies which were corrected for the exciton binding energies. The dashed-dotted lines connect experimental peak positions. To account for outgoing resonance, the energy of a LO phonon (43 meV) was subtracted from the laser energy for which the peaks occur. The theoretical lines in the lower two figures are a composition of those of the upper two graphs. ↑ and ↓ stand for spins of $+\frac{1}{2}$ and $-\frac{1}{2}$ in the conduction-band state of the transitions. Note that the experimental lines in the upper two figures were fitted to interband transitions occurring in the opposite polarization. This comes from the fact that the experiments were performed with $\mathbf{B}\|-\mathbf{z}$, whereas the calculations were done for $\mathbf{B}\|+\mathbf{z}$, which results in a change of polarizations for the transitions (Ref. 46).

with $|n,V,-\frac{3}{2}\rangle$ as the dominant contribution. Transitions between $|n,C,+\frac{1}{2}\rangle$ and $|n,V,+\frac{3}{2}\rangle$ states can be assigned to the peaks of the $\bar{z}(\sigma^-,\sigma^+)z$ spectra. The two types of transitions occur in opposite polarizations and, due to the respective valence-band contributions, the $\bar{z}(\sigma^+,\sigma^-)z$ and $\bar{z}(\sigma^-,\sigma^+)z$ spectra appear mutually exclusive, as can be observed in Fig. 4.

In the spectra with equal polarizations, we find that the experimental fan lines are in agreement with the combination of the theoretical transitions occurring for both circular polarizations. This is independent of whether the spectra are taken in $\bar{z}(\sigma^+,\sigma^+)z$- or $\bar{z}(\sigma^-,\sigma^-)z$-scattering configurations. [In the lower part of Fig. 5 the labels $n\uparrow$ ($n\downarrow$) stand for the conduction-band parts of the calculated transitions as used in the upper two fan plots. With $\uparrow$ ($\downarrow$) corresponding to spin $+\frac{1}{2}$ ($-\frac{1}{2}$) and n the usual Landau quantum number, the transitions can be readily identified.] This experimental result, which seems to be in violation of the simple selection rules for axial terms, can be understood when the valence-band mixing is considered. At the same time, a description of all steps involved in the resonant Raman processes can be obtained.

First, it is necessary to find suitable transitions for the absorption of the incident photons. This must involve states which, by either Fröhlich or deformation-potential interaction, allow for the emission of a LO phonon due to coupling to a Landau level of the real interband electronic transition which gives rise to the outgoing resonance. Since changes in the component of the angular momentum along the magnetic field of the Bloch parts of the conduction wave functions $|S\uparrow\rangle$ and $|S\downarrow\rangle$ cannot be mediated by the two types of electron-phonon interaction, we investigate Raman processes where the emission of the LO phonon must correspond to transitions between valence-band states. The calculations show that there is another type of strong interband transitions, involving the $|n,S,\pm\frac{1}{2}\rangle$ split-off-band Landau levels. Furthermore, the conduction state of an interband transition which accounts for an outgoing resonance in one polarization can only be reached by an interband transition involving split-off levels and with the opposite polarization. However, it is the admixtures to the spin-orbit split-off Landau levels which give rise to the large oscillator strengths of these transitions. This is shown in Fig. 6, which gives the eigenstates involved in a Raman process in terms of the four most dominant admixtures of the wave functions for $B=8$ T. The upper lines give the wave functions in the short notation $|n,\{C,V,S\},m_J\rangle$ whereas the full $|N_n,K^\pi,Q,P\rangle$ notation is shown below the weight coefficients. For each eigenstate the sum of the squares of these coefficients is equal to 1. The energies of the levels with respect to the top of the valence band are shown on the left-hand side of Fig. 6. The transition which occurs in outgoing resonance is found to arise from coupling between the strongest admixtures of the eigenstates at -33.65 and 1483.73 meV, leading to a transition energy of 1517.38 meV in σ^+ polarization

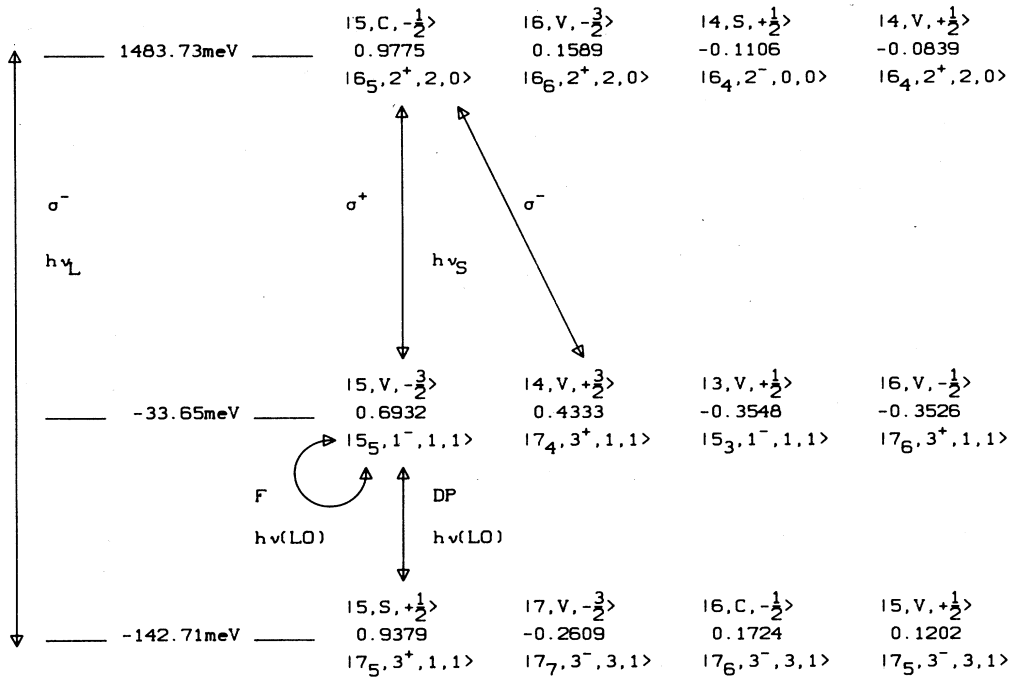

FIG. 6. Theoretical Landau levels at 8 T and transitions which contribute to a particular Raman process in the different scattering configurations for InP. The four most significant components of the wave functions are given for each level. The upper lines show the short notation of the contributing wave functions, in the middle the weighting coefficients are given, and the lower lines show the description of the states in terms of the quantum numbers $|N_n,K^\pi,Q,P\rangle$ which are explained in Sec. III. F and DP label couplings which are mediated by Fröhlich or deformation-potential electron-phonon interaction, respectively.

(theory), where the selection rules $\Delta N=+1$, $\Delta K=+1$, $\Delta Q=+1$, $\Delta P=1$, and $\Delta\pi=+1$ (Ref. 5) for transitions induced by terms of axial symmetry of the $\mathbf{k}\cdot\mathbf{p}$ Hamiltonian are obeyed. The level at -142.71 meV couples to the conduction-band state in σ^- polarization involving all the admixtures. Applying the selection rules for the electron-phonon interaction outlined in Sec. III, we realize that the two valence Landau levels couple via deformation-potential interaction, which connects the most dominant contributions of the wave functions. Thus a complete description of the Raman process in outgoing resonance has been achieved. The energy of the transition where the incident photon is absorbed is larger than the sum of energies of the Stokes photon plus the emitted LO phonon. However, because of the rather small value of the spin-orbit-coupling energy and the larger energy of the LO phonon as compared to GaAs, the energy mismatch of this virtual transition is small. This situation gives an outgoing resonant Raman process close to double resonance, where both denominators in the scattering efficiency (6) nearly vanish. Experimental evidence for this is the enormous enhancement of the scattering efficiency in the spectra taken with opposite incident and scattered circular polarizations.

When we consider the spectra for the $\bar{z}(\sigma^+,\sigma^+)z$- and $\bar{z}(\sigma^-,\sigma^-)z$-scattering configurations, it is found that the conduction-band states of the interband transitions in outgoing resonance cannot be reached from the spin-orbit split-off states in the same polarization. Another possibility for the absorption of the laser photons, however, is interband transitions from the same admixture of valence Landau levels which are involved in the outgoing resonances. Since the Fröhlich interaction leads to coupling between arbitrary Landau oscillator states n, as was mentioned in Sec. III, the emission of LO phonons by coupling within these valence-band Landau levels is possible and Raman processes occur. In order to understand, for example, why a peak observed in $\bar{z}(\sigma^+,\sigma^+)z$ can also be found in $\bar{z}(\sigma^-,\sigma^-)z$, we have to consider the components of the wave functions. In Fig. 6 it is illustrated that the strong transition for σ^+ polarization in outgoing resonance may also occur, with a weaker oscillator strength, in σ^- polarization due to coupling with the other components of the valence Landau level. Since the incident σ^- photons can be absorbed in interband transitions from both spin-orbit split-off and valence-band Landau levels, both types of electron-phonon interaction are involved in the Raman process.

These considerations explain the phenomena which occur in the different scattering configurations. The surprising fact that the peaks of both spectra with opposite circular polarizations are observed together for equal polarizations can be understood when the mixing of the valence band is considered. For a quantitative description of these resonance phenomena and of possible interference effects between Raman processes mediated by the two types of electron-phonon interaction, a theory has to be developed which takes Fröhlich and deformation-potential interaction between Landau levels into account for electronic transitions calculated with the $\mathbf{k}\cdot\mathbf{p}$ model.[35]

We have interpreted the outgoing Raman resonances in terms of interband magneto-optical transitions which are also observed in the piezomodulated reflectivity spectra (Sec. IV). From this a consistent model which describes both experiments has been proposed. It also applies to the resonant magnetopolaron effects, which in the Raman case should affect the electronic structure relevant for the transitions in outgoing resonance. As can be seen in the upper two plots of Fig. 5, there are pronounced anticrossings which occur along the fan lines of the calculated transition energies. The experimental fan lines of Fig. 5 are shown in Fig. 7 (dashed-dotted lines) after subtracting the theoretical valence-band contributions (given in Fig. 2). The straight lines of Fig. 7 correspond to the conduction-band energies calculated including corrections for the exciton binding energies. The conduction-band wave functions are given in shorthand notation and the respective valence-band levels can be found from this in analogy to Figs. 3 and 5. The anticrossings are in agreement with predictions of resonant magnetopolaron effects whenever harmonics of the cyclotron energy become equal to the energy of the LO phonon (43 meV). In addition to the anticrossings which involve the $|n=0,C,\pm\frac{1}{2};1\text{-LO}\rangle$ states, we also observe res-

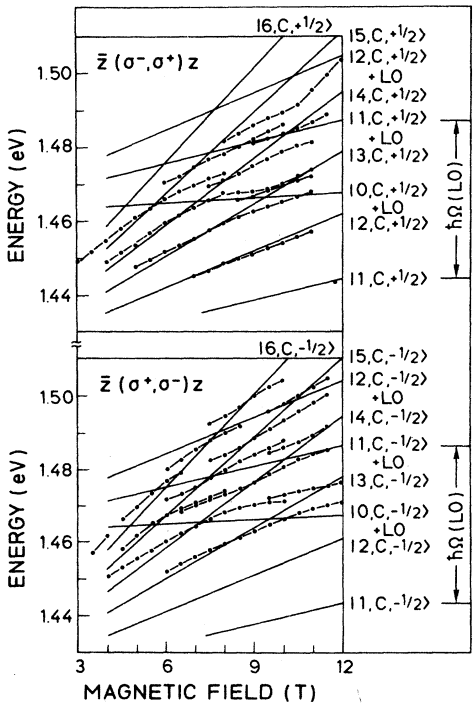

FIG. 7. Resonant magnetopolaron effects as observed in Raman scattering. Straight lines: theoretical conduction-band contributions to the interband magneto-optical transitions corrected for exciton binding energies. The transitions are labeled as explained in the text. Dashed-dotted lines: experimental peak positions corrected by 43 meV to account for the outgoing resonance and after subtraction of the theoretical valence-band contributions (see Fig. 2).

onant magnetopolaron effects where the $|n=1,C,\pm\frac{1}{2};1\text{-LO}\rangle$ and $|n=2,C,\pm\frac{1}{2};1\text{-LO}\rangle$ states contribute. In contrast to the piezoreflectance data, these anticrossings as well as the upper branches of the resonances with the $|n=0,C,\pm\frac{1}{2};1\text{-LO}\rangle$ state are readily resolved by using the magneto-Raman technique. Whereas the upper branches in the piezoreflectance experiments seem to be damped and broadened by emission of LO phonons in the k_z-dependent continuum from the lower Landau states,[39,40] the Raman efficiency seems to be less sensitive to these changes in the electronic structure. It is thus possible to study magnetopolaron resonances up to the case where the phonon energy equals 4 times the energy corresponding to the cyclotron frequency involving the $|n=6,C,-\frac{1}{2}\rangle$ and $|n=2,C,-\frac{1}{2};1\text{-LO}\rangle$ Landau states. The repulsion in energy of the anticrossings is found to be the same as estimated from piezoreflectance. An interesting effect can be seen in those regions of Fig. 7 where the lower fan line from a state with higher Landau quantum number n connects to the upper fan line of the Landau state with the next lower n. These lines were corrected for two different valence-band contributions, and thus they are clearly separated from each other in Fig. 5, where the total transition energies are plotted. This is another manifestation of the impact of valence-band mixing and underlines the necessity to take it fully into account.

VI. CONCLUSIONS

With a theoretical model for electronic states and optical transitions of III-V semiconductors in a magnetic field based on an invariant expansion for an 8×8 $\mathbf{k}\cdot\mathbf{p}$ Hamiltonian and a correction for Coulomb effects which are introduced by a variational approach, it is possible to arrive at a consistent description of the dominant features in the interband magnetopiezoreflectance spectra of InP(001). Resonant magnetopolaron effects are observed in this material, to our knowledge for the first time. With the inclusion of Fröhlich and deformation-potential electron-phonon interaction, this model can be applied to interpret the resonant enhancement of the Raman-scattering efficiency. The same interband magneto-optical transitions which dominate the piezoreflectance spectra contribute to peaks in the magneto-Raman experiments which are caused by electronic transitions in outgoing resonance. A consistent interpretation of the systematical trends for the four scattering configurations with circularly polarized light has been given. Different types of electron-phonon interaction participate in the Raman processes for spectra with opposite or equal circular polarizations for laser and Stokes photons. It is demonstrated that the mixing of the valence-band Landau levels in a magnetic field has to be fully taken into account in order to obtain a consistent description of the reflectivity and Raman experiments. Resonant magnetopolaron effects involving higher levels than the $|n=0,C,\pm\frac{1}{2};1\text{-LO}\rangle$ state are observed in the magneto-Raman experiments, a fact which highlights the usefulness and sensitivity of this modulation technique as compared to measurements of magnetoreflectivity.

ACKNOWLEDGMENTS

One of us (R.T.P.) acknowledges support from the Royal Society and the Deutsche Forschungsgemeinschaft, and expresses his thanks to the Max-Planck-Institut for hospitality. A.C. wishes to thank Generalitat Valenciana for financial support. G.A. acknowledges support from the Alexander von Humboldt Foundation. We received first-class technical assistance from H. Hirt, M. Siemers, and P. Wurster. Thanks are due to H. Krath and J. C. Maan for imaginative technical support and discussions during the reflectivity measurements at the High-Magnetic-Field Laboratory in Grenoble. F. Scholz and E. J. Thrush provided us with samples without which these experiments could not have been performed. We would also like to thank D. Heitmann for a critical reading of the manuscript.

---

*Permanent address: Department of Physics, University of Exeter, Exeter EX4 4QL, Great Britain.

†On leave from Departamento de Fisica Aplicada, Universidad Valencia, 46100 Valencia, Spain.

‡Permanent address: Institute of Semiconductor Physics, Lithuanian Academy of Sciences, 232600 Vilnius, USSR.

[1]R. L. Aggarwal, in *Semiconductors and Semimetals,* edited by R. K. Willardson and A. C. Beer (Academic, New York, 1972) Vol. 9, p. 151.

[2]J. M. Luttinger and W. Kohn, Phys. Rev. **97**, 869 (1955).

[3]J. M. Luttinger, Phys. Rev. **102**, 1030 (1956).

[4]C. R. Pidgeon and R. N. Brown, Phys. Rev. **146**, 575 (1966).

[5]H.-R. Trebin, U. Rössler, and R. Ranvaud, Phys. Rev. B **20**, 686 (1979).

[6]R. Ranvaud, H.-R. Trebin, U. Rössler, and F. H. Pollak, Phys. Rev. B **20**, 701 (1979).

[7]U. Rössler, Solid State Commun. **49**, 943 (1984).

[8]M. Braun and U. Rössler, J. Phys. C **18**, 3365 (1985).

[9]G. Ambrazevičius, M. Cardona, and R. Merlin, Phys. Rev. Lett. **59**, 700 (1987).

[10]T. Ruf, A. Cantarero, M. Cardona, J. Schmitz, and U. Rössler, in Proceedings of 19th International Conference on the Physics of Semiconductors, Warsaw, 1988 (unpublished).

[11]F. Scholz, Kristallabor, Universität Stuttgart, D-7000 Stuttgart 80, Federal Republic of Germany.

[12]E. J. Thrush, STC Technology Ltd. Essex CM17 9NA, Harlow, England.

[13]A. Gavini and M. Cardona, Phys. Rev. B **1**, 672 (1970).

[14]Piezoxide (PXE) Datenbuch, edited by Valvo, Unternehmensbereich Bauelemente der Philips GmbH, Burchardstrasse 19, 2000 Hamburg 1, Federal Republic of Germany 1986.

[15]Provided by Plano, W. Plannet GmbH, Marburger Strasse 90, 3550 Marburg 7, Federal Republic of Germany.

[16]B1827 Si photodiode with integrated FET amplifier, provided by EG&G GmbH.

[17]J. Camassel, P. Merle, L. Bayo, and H. Mathieu, Phys. Rev. B **22**, 2020 (1980).
[18]G. L. Bir and G. E. Pikus, *Symmetry and Strain-Induced Effects in Semiconductors* (Wiley, New York, 1974), Secs. 25 and 26.
[19]K. Suzuki and J. C. Hensel, Phys. Rev. B **9**, 4184 (1974).
[20]J. C. Hensel and K. Suzuki, Phys. Rev. B **9**, 4219 (1974).
[21]J. Schmitz, H.-R. Trebin, and U. Rössler (unpublished).
[22]R. J. Elliott and R. Loudon, J. Phys. Chem. Solids **15**, 196 (1960).
[23]A. Baldereschi and F. Bassani, in *Proceedings of the 10th International Conference on the Physics of Semiconductors,* Cambridge, 1970, edited by S. P. Keller, J. C. Hensel, and F. Stern (MIT Press, Cambridge, MA, 1970), p. 191.
[24]M. Altarelli and N. O. Lipari, Phys. Rev. B **9**, 1733 (1974).
[25]M. Altarelli and N. O. Lipari, Phys. Rev. B **7**, 3798 (1973).
[26]E. Jahnke and F. Emde, *Tables of Functions with Formulae and Curves* (Teubner, Leipzig, 1938).
[27]D. M. Larsen, J. Phys. Chem. Solids **29**, 271 (1968).
[28]R. M. Martin and L. M. Falicov, in *Light Scattering in Solids I,* edited by M. Cardona (Springer-Verlag, New York, 1983), p. 79.
[29]M. Cardona, in *Light Scattering in Solids II,* edited by M. Cardona and G. Guntherödt (Springer-Verlag, New York, 1982), p. 19.
[30]F. G. Bass and I. B. Levinson, Zh. Eksp. Teor. Fiz. **49**, 914 (1965) [Sov. Phys.—JETP **22**, 635 (1966)].
[31]R. C. Enck, A. S. Saleh, and H. Y. Fan, Phys. Rev. **182**, 790 (1969).
[32]S. Frota-Pessôa and R. Luzzi, Solid State Commun. **15**, 1817 (1974).
[33]A. J. C. Sampaio and R. Luzzi, Phys. Status Solidi B **91**, 305 (1979).
[34]E. O. Kane, in *Semiconductors and Semimetals,* edited by R. K. Willardson and A. C. Beer (Academic, New York, 1966), Vol. 1, p. 75.
[35]C. Trallero-Giner, T. Ruf, and M. Cardona (unpublished).
[36]E. J. Johnson and D. M. Larsen, Phys. Rev. Lett. **16**, 655 (1966).
[37]P. G. Harper, Phys. Rev. **178**, 1229 (1969).
[38]M. Nakayama, J. Phys. Soc. Jpn. **27**, 636 (1969).
[39]W. Becker, B. Gerlach, T. Hornung, and R. G. Ulbrich, in *Proceedings of the 18th International Conference on the Physics of Semiconductors, Stockholm, 1986,* edited by O. Engström (World Scientific, Singapore, 1987), p. 1713.
[40]B. D. McCombe and R. J. Wagner, in *Advances in Electronics and Electron Physics,* edited by L. Marton (Academic, New York, 1975), Vol. 38, p. 1.
[41]*Landolt-Börnstein,* edited by O. Madelung, M. Schulz, and H. Weiss (Springer-Verlag, Berlin, 1982), Vol. 17a.
[42]P. Rochon and E. Fortin, Phys. Rev. B **12**, 5803 (1975).
[43]M. Cardona, N. E. Christensen, and G. Fasol, Phys. Rev. B **38**, 1806 (1988).
[44]M. A. Alekseev, I. Ya. Karlik, D. N. Mirlin, and V. F. Sapega, Fiz. Tekh. Poluprovodn. **22**, 569 (1988) [Sov. Phys.—Semicond. **22**, 355 (1988)].
[45]F. Ancilotto, A. Fasolino, and J. C. Maan, Phys. Rev. B **38**, 1788 (1988).
[46]Note that the experimental fan lines in Ref. 10 were shifted by 53 meV, i.e., more than one LO phonon. Exciton effects would increase this shift even more. This is due to the fact that the magnetic field in the experiment was in the opposite direction with respect to the calculation (Ref. 5). A change to the complementary polarizations is thus necessary to compare experiment with theory and a fit with a shift of one LO phonon including excitonic effects can be obtained. Since the program we used is planned to be published (Ref. 21), we decided to mention this point and took care of this problem by time reversing the corresponding Bloch states (see caption of Fig. 5).
[47]M. H. Weiler, R. L. Aggarwal, and B. Lax, Phys. Rev. B **17**, 3269 (1978).